Holonomic Quantum Computation in Surface Codes

Chunfeng Wu,[1,2,*] Yimin Wang,[3] Xun-Li Feng,[4] and Jing-Ling Chen[5,†]

[1] *Science and Mathematics, Singapore University of Technology and Design, 8 Somapah Road, Singapore 487372, Singapore*

[2] *Pillar of Engineering Product Development, Singapore University of Technology and Design, 8 Somapah Road, Singapore 487372, Singapore*

[3] *Communications Engineering College, Army Engineering University, Nanjing, 210007 Jiangsu, China*

[4] *Department of Physics, Shanghai Normal University, 200234 Shanghai, China*

[5] *Theoretical Physics Division, Chern Institute of Mathematics, Nankai University, 300071 Tianjin, China*

(Received 7 August 2019; revised manuscript received 11 November 2019; published 28 January 2020)

It is well known that surface codes are favorable candidates toward realizing large-scale fault-tolerant quantum computation. While methods to reduce errors by surface codes have been well explored, it is still challenging to achieve small-enough errors as stated by the threshold theorem in practical experimental settings. This prompts the integration of surface codes and protected quantum operations to further mitigate the negative effect of errors, creating the challenge of executing protected surface codes. In this work, we propose one scheme to perform holonomic quantum operations in a physical system by use of auxiliary qubits. The system Hamiltonian describes a quantum spin model with adjustable coupling strength. Various noncommutable single-qubit and nontrivial two-qubit holonomic gates are applicable on the basis of the interaction between the auxiliary qubits and physical qubits. By considering a two-dimensional lattice of qubits, we explore the execution of surface codes. The utilization rate of physical qubits as data qubits is about 24.7% in executing the protected surface codes. Our scheme is based on an experimentally achievable Hamiltonian and thus it brings us closer to realizing protected quantum operations on quantum-error-correction codes with a modest resource.

DOI: 10.1103/PhysRevApplied.13.014055

I. INTRODUCTION

Quantum states are vulnerable to inevitable errors introduced by the interaction of the systems with their environment. That is one of the major reasons that we have not unlocked the powers promised by quantum technologies for quantum computation. To achieve large-scale quantum computation, it is of great importance to protect quantum information from the unavoidable errors during the system evolution. The threshold theorem states that if errors are sufficiently uncorrelated and small, it is possible to achieve large-scale quantum-computation tasks according to quantum-error-correction codes (QECCs) [1–3]. As stated by the theory of QECCs, a single qubit can be protected against corruption by addition of additional ancilary qubits [4]. The promise offered by QECCs to realize robust quantum-information processing has spawned extensive research on various types of QECCs [5–12]. While methods to reduce quantum errors by QECCs have been extensively developed, it remains difficult to achieve the threshold that indicates small-enough errors for fault-tolerant quantum computation in practical experimental settings, hindering the development of quantum computation with a modest resource in practice. In addition to the active technique of preserving quantum information by QECCs, there are other methods providing inherent robustness against errors through the realization of protected quantum operations. The integration of QECCs and protected quantum operations leads to a promising scalable method for quantum communication or quantum computation [13–15]. Therein arises the challenge of executing protected quantum operations on QECCs.

One effective method to achieve robust quantum operations is to use geometric properties, which are insensitive to control imprecisions [16–19]. Holonomic quantum computation (HQC) protects quantum information by applying quantum gates involving geometric properties, and hence holonomic quantum gates possess some built-in noise-resilience features [20–27]. In Refs. [26,27], HQC is generalized to nonadiabatic evolution with non-Abelian geometric phases, relaxing the requirement of a long evolution time and leading to a universal set of holonomic quantum gates. In nonadiabatic non-Abelian HQC, quantum

*chunfeng_wu@sutd.edu.sg
†chenjl@nankai.edu.cn

gates can be applied in an appropriate subspace of the system by making the system evolve along a closed path in the parameter space. Nonadiabatic non-Abelian holonomic gates have been investigated in various physical systems [28–32]. The improved approach for HQC has prompted the exploration of the combination of QECCs and protected quantum operations. Recently, Zhang *et al.* [33] showed that nonadiabatic non-Abelian holonomic quantum computation can be achieved fault tolerantly in implementing surface-code stabilizers. Nevertheless, this work provides only a mathematical model of the desired Hamiltonians for realizing single-qubit or two-qubit gates. To attain the desired Hamiltonian, specific interaction with controllable parameters is crucial, and it is a challenge to achieve such interaction in physical systems. Therefore how to perform nonadiabatic non-Abelian HQC on surface codes in a physical system is still an open problem.

Moreover, for surface codes it has been shown that the threshold of quantum-gate fidelity should be above 99.4% to achieve large-scale quantum computation [34]. The threshold provides a reference to evaluate the performance of the physical implementations of surface codes. However, as mentioned earlier, the physical realization of nonadiabatic non-Abelian HQC on surface codes with tunable qubit-qubit interaction remains unexplored. In practical experiments, imprecision in performing quantum operations stems from various sources of errors. Except for these errors, the approximation used in approaching a required effective Hamiltonian affects quantum-gate fidelity as well. Discussion of the threshold by assuming the existence of the required Hamiltonian cannot be rationalized since one may not be able to achieve the required Hamiltonian perfectly. Therefore, the execution of HQC in surface codes directly from a physical system is a problem of practical interest.

In this work, we propose a scheme to apply holonomic quantum operations in surface codes based on an experimentally achievable quantum spin model with controllable nearest-neighbor interaction. First we derive two effective Hamiltonians from the system Hamiltonian to achieve single-qubit or two-qubit holonomic quantum gates. We then consider a system of measurement qubits and data qubits placed on the nodes of a two-dimensional (2D) lattice, with auxiliary qubits placed in between the nodes. Noncommutable single-qubit and nontrivial two-qubit holonomic gates are applicable by use of the interaction between the auxiliary qubits and the measurement qubits and data qubits. On the basis of the holonomic quantum gates, we discuss the execution of surface codes. Our scheme is different from that in Ref. [33] in the following ways. Firstly, our scheme is based on an experimentally achievable Hamiltonian and therefore this paves a promising way toward realizing protected quantum operations on QECCs by near-term quantum devices. Secondly, our scheme substantially reduces the required number of auxiliary qubits to perform the holonomic quantum operations. The utilization rate of physical qubits as data qubits is about 24.7%. Lastly, we use a different way to realize single-qubit holonomic quantum gates by using auxiliary qubits.

This paper is organized as follows. In Sec. II, we present the system Hamiltonian and derive one effective Hamiltonian that can be used to realize single-qubit holonomic quantum gates by using auxiliary qubits. In Sec. III, we explore the same system Hamiltonian and derive another effective Hamiltonian for realization of two-qubit holonomic quantum gates aided by auxiliary qubits as well. In Sec. IV, we study the implementation of surface codes with the holonomic gates to further mitigate the effect of errors in quantum computation. In Sec. VI, we investigate the effect of decoherence on the execution of the holonomic gates. Finally, we conclude this paper with a discussion in Sec. V.

II. THE SYSTEM HAMILTONIAN AND SINGLE-QUBIT HOLONOMIC GATES

We consider a system of N physical qubits with controllable neighboring couplings and explore the implementation of single-qubit holonomic quantum gates. For the convenience of demonstration, we first study three of the qubits (labeled by "A," "1," and "2"). Qubits 1 and 2 describe the measurement and data qubits needed for surface codes, and qubit A is the auxiliary qubit required for implementation of holonomic quantum operations on normal qubits 1 and/or 2. It is easy to generalize the following investigations to any three qubits. The three-qubit Hamiltonian is

$$H = \sum_{j=A,1,2}\left(\frac{\epsilon_j}{2}\sigma_z^j + \frac{\Delta_j}{2}\sigma_x^j\right) + J_{A1}\sigma_x^A\sigma_x^1 + J_{A2}\sigma_x^A\sigma_x^2 + \frac{\varepsilon_A}{2}\sin(\omega_A t + \phi_A)\sigma_z^A, \tag{1}$$

where ϵ_j and Δ_j are the parameters describing the energy of each qubit, σ_α^j $(\alpha = x, y, z)$ are the α components of the j th Pauli matrix, J_{ij} is the coupling strength of qubits i and j, ε_A, ω_A, and ϕ_A are, respectively, the driving strength, frequency, and phase of the external driving applied on qubit A.

We first apply local quantum operations on qubits 1 and 2 such that the system Hamiltonian is revised as

$$H_r = \frac{\epsilon_1'}{2}\sigma_z^1 + \frac{\epsilon_2'}{2}\sigma_z^2 + \frac{\epsilon_A}{2}\sigma_z^A + \frac{\Delta_A}{2}\sigma_x^A + \sum_{j=1,2} J_{Aj}\sigma_x^A(\sin\theta\sigma_x^j - \cos\theta\sigma_z^j) + \frac{\varepsilon_A}{2}\sin(\omega_A t + \phi_A)\sigma_z^A, \tag{2}$$

where $\epsilon_i' = \sqrt{(\epsilon_i)^2 + (\Delta_i)^2}$ and $\tan\theta = -\epsilon_j/\Delta_j$.

To apply single-qubit holonomic quantum gates, we adjust $J_{A2}=0$. We then move to the rotating frame defined by the time-dependent transformation $\mathcal{U}(t)=\mathcal{U}_1(t)\mathcal{U}_2(t)$, with $\mathcal{U}_1(t)=\exp\left\{-i\left[(\epsilon_1'/2)\sigma_z^1+(\epsilon_2'/2)\sigma_z^2+(\epsilon_A/2)\sigma_z^A\right]t\right\}$ and $\mathcal{U}_2(t)=\exp\left[i(\alpha_A/2)\cos(\omega_A t+\phi_A)\sigma_z^A\right]$, where $\alpha_A=\varepsilon_A/\omega_A$, and apply the Jacobi-Anger expansion [35], $e^{i\alpha_A\cos(\omega_A t+\phi_A)}=\sum_{l=-\infty}^{+\infty}i^l J_l(\alpha_A)e^{il(\omega_A t+\phi_A)}$, where $J_l(\alpha_m)$ is the Bessel function of the first kind. If we set $\epsilon_1'=2\epsilon_A=2\omega_A$, $\Delta_A=2J_{A1}\cos\theta$, $\phi_A=-\pi/2-\varphi$, and $\epsilon_A\gg\{J_{A1},\Delta_A\}$, higher-order terms can be ignored according to the rotating-wave approximation (RWA). Therefore, we obtain the effective Hamiltonian:

$$H_{\rm eff}=Je^{-i\varphi}\sigma_+^A\sigma_-^1+\Delta e^{i\varphi}\sigma_+^A(\mathcal{I}_2-\sigma_z^1)+\text{H.c.}, \quad (3)$$

where $\mathcal{I}_2$ is the identity matrix acting on qubit 1, $J=J_{A1}\sin\theta J_1(-\alpha_A)$, $\Delta=J_{A1}\cos\theta J_1(\alpha_A)$, and $\sigma_\pm^j=\frac{1}{2}(\sigma_x^j\pm i\sigma_y^j)$.

We now elaborate on the implementation of single-qubit holonomic gates based on the effective Hamiltonian. The effective Hamiltonian is equivalent to the following form up to a global phase:

$$H_{\rm eff}=\Omega\left[\sin\left(\frac{\vartheta}{2}\right)e^{-i2\varphi}|01\rangle\langle 10| + \cos\left(\frac{\vartheta}{2}\right)|01\rangle\langle 11|+\text{H.c.}\right], \quad (4)$$

where $\Omega=\sqrt{J^2+(2\Delta)^2}$, $\vartheta=2\tan^{-1}(J/2\Delta)$, and $|ij\rangle=|i\rangle_A|j\rangle_1$. We define two subspaces, $\mathcal{S}_0=\{|00\rangle,|01\rangle\}$ and $\mathcal{S}_1=\{|10\rangle,|11\rangle\}$. The projection operators for $\mathcal{S}_j$ are $P_{\mathcal{S}_0}=|00\rangle\langle 00|+|01\rangle\langle 01|$ and $P_{\mathcal{S}_1}=|10\rangle\langle 10|+|11\rangle\langle 11|$. Initially, quantum information is stored in subspace $\mathcal{S}_1$. When $H_{\rm eff}$ is applied, the subspace is driven out of $\mathcal{S}_1$. This is because $H_{\rm eff}$ can be recast as $|01\rangle$ coupled with state $|b\rangle=e^{i2\varphi}\sin(\vartheta/2)|10\rangle+\cos(\vartheta/2)|11\rangle$ and decoupled from state $|d\rangle=e^{-i2\varphi}\sin(\vartheta/2)|11\rangle-\cos(\vartheta/2)|10\rangle$. Driven by $H_{\rm eff}$, we obtain the Rabi oscillation between states $|b\rangle$ and $|01\rangle$ with the Rabi frequency of Ω. If we control the parameter such that $\int_0^\tau\Omega\,\mathbf{d}t=\pi$, the system states return to subspace $\mathcal{S}_1$. Therefore, the evolution operator according to $H_{\rm eff}$ is of the following form:

$$U(\tau)=\begin{pmatrix}1&0&0&0\\0&-1&0&0\\0&0&\cos\vartheta&-\sin\vartheta e^{i2\varphi}\\0&0&-\sin\vartheta e^{-i2\varphi}&-\cos\vartheta\end{pmatrix}, \quad (5)$$

written in the basis of $\{|00\rangle,|01\rangle,|10\rangle,|11\rangle\}$. Equivalently,

$$U(\tau)=|0\rangle_A\langle 0|\otimes U_0(\tau)+|1\rangle_A\langle 1|\otimes U_1(\tau), \quad (6)$$

where $U_0(\tau)=\sigma_z$ and $U_1(\tau)=\mathbf{n}\cdot\boldsymbol{\sigma}$, where $\mathbf{n}=(-\sin\vartheta\cos 2\varphi,\sin\vartheta\sin 2\varphi,\cos\vartheta)$ and $\boldsymbol{\sigma}=(\sigma_x,\sigma_y,\sigma_z)$ are the Pauli operators.

It is clear that noncommuting single-qubit quantum gates acting on qubit 1 can be achieved on the basis of $U_1(\tau)$ by varying ϑ and φ. To see that $U_1(\tau)$ describes a nonadiabatic holonomic quantum gate acting on $\mathcal{S}_1$, we recall the fact that the system states undergo a cyclic evolution within $\mathcal{S}_1$ at $t=\tau$, and hence one condition to guarantee the nonadiabatic holonomic quantum gates is satisfied. The time-dependent projection operator is $P_{\mathcal{S}_j}(t)=U(t)P_{\mathcal{S}_j}U^\dagger(t)$, where $U(t)$ is the evolution operator according to $H_{\rm eff}$. It is easy to find $P_{\mathcal{S}_j}(t)H_{\rm eff}P_{\mathcal{S}_j}(t)=U(t)P_{\mathcal{S}_j}H_{\rm eff}P_{\mathcal{S}_j}U^\dagger(t)=0$, and this result shows that the evolution is geometric [26–28].

In the following, we check the validity of the approximation in deriving $H_{\rm eff}$ numerically. We choose $|\psi(0)\rangle=(1/\sqrt{|a_1|^2+|a_2|^2})(a_1|10\rangle+a_2|11\rangle)$ as the initial state. We denote $|\psi(\tau)\rangle$ as the evolution states governed by the original Hamiltonian and $|\psi'(\tau)\rangle=U(\tau)|\psi(0)\rangle$, respectively. Let $F(\tau)=|\langle\psi(\tau)|\psi'(\tau)\rangle|^2$ be the fidelity for the states $|\psi(\tau)\rangle$ and $|\psi'(\tau)\rangle$. We numerically find the average fidelity $\overline{F}$ at $\tau=\pi/\Omega$ by randomly selecting 50 initial states by choosing random $a_j=a_j^r+ia_j^c$, where a_j^r and a_j^c are from a uniform distribution with parameters $[-1/2,1/2]$, with the following parameters: $\epsilon_A=2\pi\times 8$ GHz, $\epsilon_1'=2\epsilon_2'=2\epsilon_A$, $\omega_A=\epsilon_A$, $\varepsilon_A=0.8\omega_A$, $J_{A1}=0.008\epsilon_1'$, and $\Delta_A=2J_{A1}\cos\theta$. Specifically, we choose $\theta=0$ such that $\vartheta=0$ to achieve a single-qubit gate $U_{1,1}(\tau)=\sigma_z$ and obtain average fidelity $\overline{F}_1=0.9989$. We find another average fidelity $\overline{F}_2=0.997$ when $\theta=\arctan 2$ such that $\vartheta=-\pi/2$ and $\varphi=0$, and this gate is $U_{1,2}(\tau)=\sigma_x$. We then change the parameters to realize a single-qubit gate $U_{1,3}(\tau)=\sigma_y$ with $\theta=-\arctan 2$ such that $\vartheta=\pi/2$ and $\varphi=\pi/4$. The corresponding average fidelity $\overline{F}_3=0.9975$. Another example is the Hadamard gate $U_{1,4}(\tau)=H$ when $\theta=\arctan[2\tan(\pi/8)]$ such that $\vartheta=-\pi/4$ and $\varphi=0$. We get average fidelity $\overline{F}_4=0.9988$. Therefore, we obtain excellent average gate fidelities for various noncommutable single-qubit gates. In other words, it can be inferred from the numerical results that the effective Hamiltonian (4) approximates the original time-dependent Hamiltonian very well by our choosing appropriate parameters.

III. THE SYSTEM HAMILTONIAN AND TWO-QUBIT HOLONOMIC GATES

To achieve universal quantum gates acting on surface codes we explore the implementation of a nontrivial two-qubit gates as follows. In this case, we set $\varepsilon_A=0$ and $J_{A2}\neq 0$ in Hamiltonian (2). Rotating the frame with respect to $\mathcal{U}_1(t)=\exp\left\{-i\left[(\epsilon_1'/2)\sigma_z^1+(\epsilon_2'/2)\sigma_z^2+(\epsilon_A/2)\sigma_z^A\right]t\right\}$, and choosing $\epsilon_j'=\epsilon_A$ and $\epsilon_A\gg\{J_{Aj},\Delta_A\}$, we can ignore higher-order terms and obtain the following

effective Hamiltonian according to the RWA:

$$H'_{\text{eff}} = \Omega_1 \sigma_+^A \sigma_-^1 + \Omega_2 \sigma_+^A \sigma_-^2 + \text{H.c.}, \tag{7}$$

where $\Omega_j = J_{Aj} \sin\theta$.

Written in the three-qubit basis of $\{|ijk\rangle = |i\rangle_A |j\rangle_1 |k\rangle_2\}$, the above effective Hamiltonian is equivalent to

$$\begin{aligned} H'_{\text{eff}} = {} & \Omega' \left[\sin\left(\frac{\vartheta'}{2}\right) |011\rangle\langle 101| + \cos\left(\frac{\vartheta'}{2}\right) |011\rangle\langle 110| \right] \\ & + \Omega' \left[\sin\left(\frac{\vartheta'}{2}\right) |100\rangle\langle 010| + \cos\left(\frac{\vartheta'}{2}\right) |100\rangle\langle 001| \right] \\ & + \text{H.c.}, \end{aligned} \tag{8}$$

where $\Omega' = \sqrt{\Omega_1^2 + \Omega_2^2}$ and $\vartheta' = 2\tan^{-1}(\Omega_1/\Omega_2)$. At $T = \pi/\Omega'$, the evolution operator of H'_{eff} has two invariant subspaces, $\mathcal{S}'_0 = \{|000\rangle, |001\rangle, |010\rangle, |011\rangle\}$ and $\mathcal{S}'_1 = \{|100\rangle, |101\rangle, |110\rangle, |111\rangle\}$. This is because in either subspace the system undergoes cyclic evolution when $T = \pi/\Omega'$, similar to the reasoning in Sec. II. We define the projection operators $P_{\mathcal{S}'_0} = |000\rangle\langle 000| + |001\rangle\langle 001| + |010\rangle\langle 010| + |011\rangle\langle 011|$ and $P_{\mathcal{S}'_1} = |100\rangle\langle 100| + |101\rangle\langle 101| + |110\rangle\langle 110| + |111\rangle\langle 111|$ for subspaces $\mathcal{S}'_0$ and $\mathcal{S}'_1$, respectively. We observe that $P_{\mathcal{S}'_j}(t) H'_{\text{eff}} P_{\mathcal{S}'_j}(t) = U'(t) P_{\mathcal{S}'_j} H'_{\text{eff}} P_{\mathcal{S}'_j} U'^{\dagger}(t) = 0$, where $U'(t)$ is the evolution operator according to H'_{eff} and $P_{\mathcal{S}'_j}(t) = U'(t) P_{\mathcal{S}'_j} U'^{\dagger}(t)$. The results tell us that nonadiabatic quantum holonomy acting on $\mathcal{S}'_j$ can be achieved, and hence the evolution operator from H'_{eff} defines two-qubit holonomic gates acting in subspaces $\mathcal{S}'_0$ and $\mathcal{S}'_1$ [26,27,31,33].

We use $U'_j(T)$ to describe the evolution operators in the subspaces and we find

$$U'_0(T) = \begin{pmatrix} 1 & 0 & 0 & 0 \\ 0 & -\cos\vartheta' & -\sin\vartheta' & 0 \\ 0 & -\sin\vartheta' & \cos\vartheta' & 0 \\ 0 & 0 & 0 & -1 \end{pmatrix},$$

$$U'_1(T) = \begin{pmatrix} -1 & 0 & 0 & 0 \\ 0 & \cos\vartheta' & -\sin\vartheta' & 0 \\ 0 & -\sin\vartheta' & -\cos\vartheta' & 0 \\ 0 & 0 & 0 & 1 \end{pmatrix}. \tag{9}$$

According to the above evolution operators in each subspace, the total evolution operator takes the following form:

$$U'(T) = |0\rangle_A\langle 0| \otimes U'_0(T) + |1\rangle_A\langle 1| \otimes U'_1(T). \tag{10}$$

It is easy to see that $U'_j(T)$ are two-qubit gates acting on qubits 1 and 2. If we consider the case that qubit A is initially in ground state $|1\rangle$, we obtain the two-qubit gate $U'_1(T)$ dependent on the values of ϑ'.

Similarly, we check the validity of the approximation involved in the derivation of the effective Hamiltonian (7) in a numerical way. We choose $|\Psi(0)\rangle = \left(1/\sqrt{\sum_{j=1}^4 |a_j|^2}\right)(a_1|100\rangle + a_2|101\rangle + a_3|110\rangle + a_4|111\rangle)$ as the initial states, where $a_j = a_j^r + i a_j^c$, where a_j^r and a_j^c are from a uniform distribution with parameters $[-1/2, 1/2]$. We denote $|\Psi(T)\rangle$ as the evolution states governed by the original Hamiltonian and $|\Psi'(T)\rangle = U'_1(T)|\Psi(0)\rangle$, respectively. Let $F'(T) = |\langle\Psi(T)|\Psi'(T)\rangle|^2$ be the fidelity for the states $|\Psi(T)\rangle$ and $|\Psi'(T)\rangle$. We numerically find average fidelity $\overline{F'}$ at $T = \pi/\Omega'$ by randomly selecting 50 initial states with the parameters $\epsilon_A = 2\pi \times 8$ GHz and $\epsilon'_1 = \epsilon'_2 = \epsilon_A$, and we vary J_{A1} and J_{A2}. First we select $\Delta_A = 0.001\epsilon'_1$, $\theta = \pi/3$, and $J_{A1} = J_{A2} = 0.008\epsilon'_1$ such that $\vartheta' = \pi/2$, and the achieved gate is $U'_{1,1}(T) = -U_{\text{sz}}$ (SZ relates to the name of the gate, see [33]) with average fidelity $\overline{F'}_1 = 0.9996$, where

$$U_{\text{sz}} = \begin{pmatrix} 1 & 0 & 0 & 0 \\ 0 & 0 & 1 & 0 \\ 0 & 1 & 0 & 0 \\ 0 & 0 & 0 & -1 \end{pmatrix}. \tag{11}$$

Furthermore, we change the parameters and find another average fidelity $\overline{F'}_2 = 0.9992$ when $J_{A1} = \tan(\pi/8) J_{A2} = 0.008\epsilon'_1$ such that $\vartheta' = \pi/4$, and this gate is of the following form:

$$U'_{1,2}(T) = \begin{pmatrix} -1 & 0 & 0 & 0 \\ 0 & \frac{\sqrt{2}}{2} & -\frac{\sqrt{2}}{2} & 0 \\ 0 & -\frac{\sqrt{2}}{2} & -\frac{\sqrt{2}}{2} & 0 \\ 0 & 0 & 0 & 1 \end{pmatrix}. \tag{12}$$

The excellent average gate fidelities for different two-qubit gates demonstrate that the effective Hamiltonian (7) is very close to the original time-dependent Hamiltonian with proper parameters. As shown by the numerical results, it is clear that two-qubit-gate fidelities are higher than one-qubit-gate fidelities. The numerical results can be understood in the following way. When we derive effective Hamiltonian (3) for realization of one-qubit gates, external driving with coefficient ε_A is needed to achieve the required terms for holonomic quantum gates, while when we derive effective Hamiltonian (7) for realization of two-qubit gates, we let the coefficient ε_A equal zero to remove the external driving. In the absence of the external driving, fewer higher-order terms are ignored according to the RWA in deriving Eq. (7) than in deriving Eq. (3). Moreover, the evolution time required to achieve a one-qubit gate is longer than that required to achieve a two-qubit gate due to the term $J_1(\alpha_A)$, which is around 0.37 according to the parameters chosen. The longer the evolution time, the

worse the approximation is, and therefore two-qubit-gate fidelities are higher than one-qubit-gate fidelities.

Finally we have achieved the implementation of noncommutable single-qubit and nontrivial two-qubit holonomic quantum operations from the system Hamiltonian (2). According to universal quantum computation, any holonomic quantum operations should be executable by use of the combination of single-qubit and two-qubit gates.

IV. THE IMPLEMENTATION OF HOLONOMIC SURFACE CODES

Surface codes are desirable candidates for achieving large-scale fault-tolerant quantum computation [8]. The stabilizers of surface codes are usually described by multiqubit observables, and therefore it is challenging to measure them in practical experiments since multiqubit interactions rarely naturally exist in physical systems. Nevertheless, by use of measurement qubits, one can measure multiqubit observables by using quantum circuits in terms of single-qubit and two-qubit gates acting on measurement and data qubits based on nearest-neighbor interactions [8]. Therefore surface codes are commonly investigated via a 2D lattice of qubits, including measurement and data qubits [8]. The measurement qubits (described by "Z" or "X") have the corresponding stabilizer $\sigma_z^{i_1}\sigma_z^{i_2}\sigma_z^{i_3}\sigma_z^{i_4}$ or $\sigma_x^{i_1}\sigma_x^{i_2}\sigma_x^{i_3}\sigma_x^{i_4}$ acting on the four nearest data qubits i_1, i_2, i_3, and i_4. At the boundary of the lattice, the stabilizers are revised to have three Pauli operators operating on the three nearest data qubits.

It was shown that the threshold of quantum gate fidelity should be above 99.4% [34] to achieve large-scale quantum computing based on surface codes. This result promoted studies exploring stabilizers by use of holonomic quantum operations to reduce the bothersome effect of noise [15,33]. In the literature, mathematical models of Hamiltonians required for implementation of nonadiabatic non-Abelian holonomic quantum gates have been investigated, but the Hamiltonians are not from practical physical systems. Moreover, controllable qubit-qubit interaction is crucial for execution of the surface codes according to their encoding quantum circuits since the encoding circuits rely on single-qubit and two-qubit gates. So it is important to adjust qubit-qubit interaction step by step to achieve the gates. Discussion of physical implementation of the surface codes with controllable qubit-qubit interaction remains unexplored.

In this section, we study the execution of holonomic surface codes based on the single-qubit and two-qubit holonomic quantum gates obtained from an actual system Hamiltonian. We consider a 2D lattice of qubits, including measurement qubits, data qubits, and type-I and type-II auxiliary qubits as shown in Fig. 1(a). The qubits are coupled as indicated by line segments connecting different qubits. When single-qubit operations are performed, type-I auxiliary qubits are used and they are in their ground states during evolution. For implementation of two-qubit operations, both types of auxiliary qubits are needed, where type-I auxiliary qubits are in their ground states.

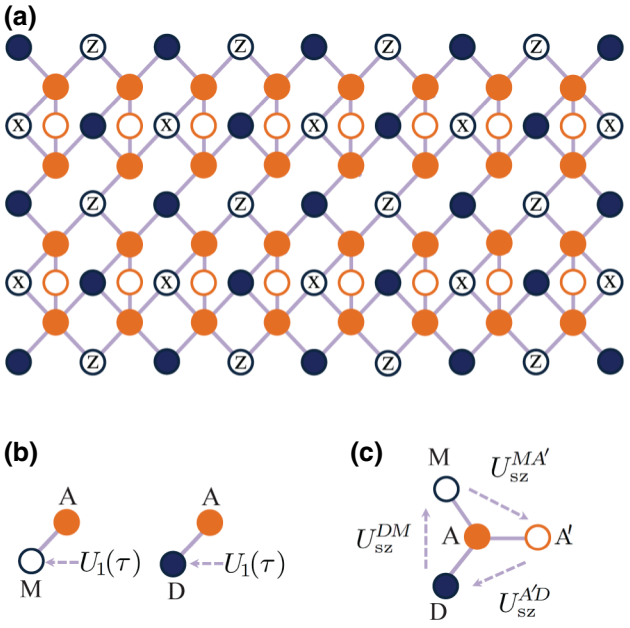

FIG. 1. (a) A 2D lattice of qubits for surface codes. Solid dark-blue dots represent data qubits, hollow dark-blue dots represent measurement qubits, and solid and hollow orange dots represent as type-I and type-II auxiliary qubits, respectively. The line segments between qubits indicate controllable qubit-qubit couplings. (b) The implementation of single-qubit holonomic quantum gates on a measurement qubit or a data qubit. (c) The implementation of a SWAP gate on a pair of measurement and data qubits.

According to the quantum circuits based on single-qubit or two-qubit gates, syndrome measurements can be performed by the action of Hadamard and controlled NOT (CNOT) gates on measurement and data qubits, followed by measurement of measurement qubits in a proper basis to get the error syndrome. Here we show that the physical realization of syndrome measurements by use of holonomic quantum operations can be achieved on the basis of the discussions in the previous sections. As demonstrated in Fig. 1(a), the measurement qubits are connected to at least one type-I auxiliary qubit, and therefore various single-qubit holonomic gates $U_1(\tau)$ are realizable according to Eq. (5); see Fig. 1(b). Specifically, a holonomic Hadamard gate can be applied by choosing the corresponding θ to be $\arctan[2\tan(\pi/8)]$. Moreover, we ensure that any pair of nearest-neighbor measurement or data qubits are connected to one type-I auxiliary qubit that is at the same time linked to one type-II auxiliary qubit. From Eq. (10), we know when $\vartheta' = \pi/2$ that we have the two-qubit holonomic gate U_{sz}^{12}, where superscript 12 means the operation is acting on qubits 1 and

2. Similarly, when we consider another three-qubit interaction with type-I and type-II auxiliary qubits by adjusting qubit-qubit couplings, we can find $U_{\rm sz}$ acting on one type-II auxiliary qubit and one normal qubit (either a measurement qubit or a data qubit) and meanwhile the type-I auxiliary qubit is in its ground state. As shown in Ref. [33], controlled-Z and CNOT gates acting on measurement and data qubits can be applied according to the combinations of the above-mentioned quantum operations. As illustrated in Fig. 1(c), a SWAP gate can be implemented on the measurement and data qubits in the following way: $U^{MD}_{\rm SWAP} = U^{A'D}_{\rm sz} U^{DM}_{\rm sz} U^{MA'}_{\rm sz}$. A controlled-$Z$ gate is then $U^{MD}_{\rm cZ} = U^{MD}_{\rm sz} U^{MD}_{\rm SWAP}$, and hence a CNOT gate is $U^{MD}_{\rm CNOT} = (\mathcal{I}_2 \otimes H) U^{MD}_{\rm cZ} (\mathcal{I}_2 \otimes H)$. The average fidelities are $(\overline{F'}_1)^4 \sim 0.998$ and $(\overline{F}_4)^2 (\overline{F'}_1)^4 \sim 0.996$, respectively. Hence, we have successfully achieved single-qubit and two-qubit holonomic quantum gates operating on measurement and data qubits, and as a result the implementation of syndrome measurements according to the quantum circuits. Thus, the error syndromes can be extracted on the basis of the protected quantum operations and then quantum error correction can be performed on data qubits accordingly by use of single-qubit holonomic gates as discussed in Sec. II.

Given the holonomic syndrome measurements, surface codes can be initialized in logic $|0\rangle$ or logic $|+\rangle$ states [8, 36]. For example, logic $|0\rangle$ can be obtained by preparing all physical qubits in $|0\rangle$ states followed by a sequence of syndrome measurements. Moreover, quantum operations on multiple logic qubits are shown to be executable through a lattice surgery procedure [36]. The procedure depends on proper syndrome measurements and single-qubit and two-qubit quantum gates acting on physical qubits with nearest-neighbor interactions. Therefore, universal quantum computation on logic qubits can be implemented with the holonomic quantum gates explored in Secs. II and III. As a result, both the initialization of logic qubits and quantum operations on logic qubits can be protected by the holonomic quantum operations.

Our scheme can be readily explored in a superconducting system, and in the following we briefly focus on a minimal model for superconducting qubits, which possess good controllability. We take the superconducting charge-qubit architecture shown in Fig. 2 as an illustration, where a pair of nearest-neighbor charge qubits are coupled by a large Josephson junction acting as an effective inductance. Each charge qubit is a Cooper-pair box consisting of a dc superconducting quantum-interference device (SQUID) formed by a superconducting island connected to two Josephson junctions, and is biased by an applied voltage V_{gj} through a gate capacitance C_{gj}, and each SQUID is pierced by a magnetic flux Φ_{qj}. As described in Eq. (1), the resulting system Hamiltonian is of $\sigma_x\sigma_x$-type coupling between qubit 1 (qubit2) and qubit A [37–39], and the corresponding qubit parameters and qubit-qubit coupling strength are

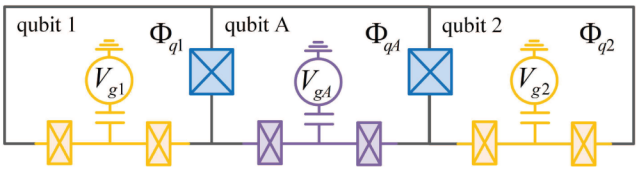

FIG. 2. Coupled array for superconducting qubits. Qubit 1 (qubit 2) (orange) is coupled to the auxiliary qubit A (purple) by a large Josephson junction with coupling energy E^c_{Jj} (crossed rectangle in blue). Φ_{qj} is the flux applied to each qubit loop.

adjustable; that is, $\epsilon_j = E_{cj}(1 - C_{gj} V_{gj}/e)$ is controllable via the gate voltage V_{gj}; $\Delta_j = E_{J0,j} \cos(\pi \Phi_{qj}/\Phi_0)$ and $J_{Aj} = L_{Jj} (\pi E_{J0,j}/\Phi_0)^2 \sin(\pi \Phi_{qA}/\Phi_0) \sin(\pi \Phi_{qj}/\Phi_0)$ can be controlled by the applied local fluxes Φ_{qj}. Here $E_{cj} = e^2/C_{Jj}$ and $L_{Jj} = \Phi_0/2\pi I^c_j$, where $I^c_j = 2\pi E^c_{Jj}$ and Φ_0 is the flux quantum. By periodically modulating the applied gate voltage for qubit A [i.e., choosing $V'_{gA} = V_{gA} + V'_{gA} \sin(\omega_A t + \phi_A)$], we arrive at the Hamiltonian (1) with $\varepsilon_A = -EcC_{gA} V'_{gA}/e$. Hence, our scheme to investigate protected surface codes is possibly executable in the system.

Zhang *et al.* [33] proposed using auxiliary qubits rather than auxiliary levels to achieve quantum holonomy. Our scheme also uses auxiliary qubits in implementing holonomic quantum gates. The merit of using auxiliary qubits is to reduce the decoherence effect due to higher levels. The differences between Ref. [33] and our scheme are threefold:

(a) Our scheme is the physical realization of executing surface codes, while Ref. [33] provides only a mathematical model of the Hamiltonian;

(b) We substantially reduce the number of auxiliary qubits as compared with Ref. [33], losing the requirement of a resource for implementing the protected surface codes. In our scheme as illustrated in Fig. 1, there are 23 data qubits, 32 type-I auxiliary qubits, 16 type-II auxiliary qubits, and 22 measurement qubits. This implies that roughly 24.7% of the physical qubits are used as data qubits, while in Fig. 1(c) of Ref. [33] the utilization rate of physical qubits as data qubits is about 11.7%. Therefore, the number of required auxiliary qubits is largely reduced in our scheme. This is indeed a desirable saving of resources in realistic experimental settings.

(c) We realize single-qubit gates in a different way.

V. THE EFFECT OF DECOHERENCE

In a practical study, decoherence due to the interaction between the system and its environment cannot be avoided. We study the performance of the holonomic quantum operations in the presence of different noises in this section. The evolution of the system is determined by the following

TABLE I. The effect of qubit dephasing on the performance of holonomic gates.

Fidelity	$\gamma_z = 0.6 \times 10^{-5}\epsilon_A$	$\gamma_z = 2 \times 10^{-5}\epsilon_A$	$\gamma_z = 2 \times 10^{-4}\epsilon_A$
$\overline{F}_{1,\mathrm{de}}$	0.9981	0.9963	0.9740
$\overline{F}_{2,\mathrm{de}}$	0.9951	0.9906	0.9360
$\overline{F}_{3,\mathrm{de}}$	0.9957	0.9915	0.9405
$\overline{F}_{4,\mathrm{de}}$	0.9976	0.9949	0.9613
$\overline{F'}_{1,\mathrm{de}}$	0.9964	0.9889	0.9061
$\overline{F'}_{2,\mathrm{de}}$	0.9973	0.993	0.9423

master equation:

$$\frac{d\rho}{dt} = -i[H,\rho] + \sum_{k=z,-} \gamma_k \left(\mathcal{L}_k \rho \mathcal{L}_k^\dagger - \frac{1}{2}\mathcal{L}_k^\dagger \mathcal{L}_k \rho - \frac{1}{2}\rho \mathcal{L}_k^\dagger \mathcal{L}_k \right), \tag{13}$$

where γ_z and γ_- are the decay rates of qubit dephasing and relaxation, respectively, and $\mathcal{L}_z = \sum_{j=A,1,2} \sigma_z^j$, $\mathcal{L}_- = \sum_{j=A,1,2} \sigma_-^j$, where $\sigma_-^j = \frac{1}{2}(\sigma_x^j - i\sigma_y^j)$.

In the presence of noise, the fidelities $\overline{F}_{i,\mathrm{de}} = \mathrm{Tr}[\rho\rho']$ $(i = 1,\ldots,4)$ of single-qubit holonomic gates and $\overline{F^{(\prime)}}_{i,\mathrm{de}} = \mathrm{Tr}[\rho\rho']$ $(i = 1,2)$ of two-qubit holonomic gates are calculated with ρ an ρ' being the density matrices of a three-qubit system in the case without and with decoherence, respectively. The numerical results are listed in Tables I and II for different decay rates. We study how qubit dephasing and relaxation noises affect the performance of the holonomic gates individually. We choose $\gamma_- = 0$ but vary γ_z first to realize different quantum gates; the fidelities are shown in Table I. In a similar way, we calculate the average fidelities by selecting $\gamma_z = 0$ but varying γ_- to implement various quantum gates; the fidelities are listed in Table II. It is illustrated by the numerical results that the gate fidelities are a little bit more robust against qubit relaxation than qubit dephasing. When the decay rates are increased, the gate fidelities are largely affected by the noise as compared with the fidelities in the absence of decoherence. This suggests that our scheme is vulnerable to large decay rates.

TABLE II. The effect of qubit relaxation on the performance of holonomic gates.

Fidelity	$\gamma_- = 0.6 \times 10^{-5}\epsilon_A$	$\gamma_- = 2 \times 10^{-5}\epsilon_A$	$\gamma_- = 2 \times 10^{-4}\epsilon_A$
$\overline{F}_{1,\mathrm{de}}$	0.9978	0.9953	0.9636
$\overline{F}_{2,\mathrm{de}}$	0.9960	0.9935	0.9628
$\overline{F}_{3,\mathrm{de}}$	0.9963	0.9936	0.9600
$\overline{F}_{4,\mathrm{de}}$	0.9976	0.9950	0.9627
$\overline{F'}_{1,\mathrm{de}}$	0.9979	0.9941	0.9477
$\overline{F'}_{2,\mathrm{de}}$	0.9983	0.9962	0.9705

VI. CONCLUSION

We present a scheme to realize holonomic quantum gates in a physical system with adjustable qubit-qubit couplings. With use of the controllable parameters describing qubit energy and qubit-qubit coupling, we can derive two effective Hamiltonians that lead to single-qubit and two-qubit holonimic gates from the evolution of the system. Numerically using a set of physical parameters, we show that the holonomic gates can be implemented with high fidelities. By considering a 2D lattice of qubits, we explore the implementation of surface codes based on the holonomic quantum gates by using two types of auxiliary qubits. The holonomic quantum gates acting on measurement and/or data qubits are achieved by use of auxiliary qubits rather than auxiliary energy levels, and hence the decoherence effect due to higher energy levels can be reduced. As a result of the geometric nature of the holonomic gates, applying them in surface code helps to further mitigate the negative effect of noise. The integration of the surface codes and holonomic quantum computation in this work offers advantages over the schemes in the literature. On one hand, we provide a practical scheme in a physical system and the scheme is possibly experimentally achievable. On the other hand, the number of required auxiliary qubits is largely reduced, losing the requirement of a resource. We also demonstrate numerically that in the presence of decoherence from the coupling of the system to its environment, our scheme is more resilient to qubit relaxation as compared with qubit dephasing, and is susceptible to noise when the decay rates are increased.

ACKNOWLEDGMENTS

We appreciate valuable discussions with Y. Ouyang. Y.M.W. was supported by the National Natural Science Foundation of China (Grant No. 11404407). J.L.C. was supported by the National Natural Science Foundation of China (Grant No. 11875167).

[1] D. P. DiVincenzo and P. W. Shor, Fault-Tolerant Error Correction with Efficient Quantum Codes, Phys. Rev. Lett. **77**, 3260 (1996).
[2] D. Aharonov and M. Ben-Or, in *Proc. 29th Annual ACM Symposium on the Theory of Computation* (ACM Press, New York, 1997), p. 176.
[3] E. Knill, Quantum computing with realistically noisy devices, Nature (London) **434**, 39 (2005).
[4] M. A. Nielsen and I. L. Chuang, *Quantum Computation and Quantum Information* (Cambridge University Press, Cambridge, 2000).
[5] H. Ollivier and J.-P. Tillich, Description of a Quantum Convolutional Code, Phys. Rev. Lett. **91**, 177902 (2003).

[6] Y. Ouyang, Concatenated quantum codes can attain the quantum Gilbert–Varshamov bound, IEEE Trans. Inf. Theory **60**, 3117 (2014).

[7] H. Bombin, Topological subsystem codes, Phys. Rev. A **81**, 032301 (2010).

[8] A. G. Fowler, M. Mariantoni, J. M. Martinis, and A. N. Cleland, Surface codes: Towards practical large-scale quantum computation, Phys. Rev. A **86**, 032324 (2012).

[9] S. Bravyi and J. Haah, Quantum Self-Correction in the 3D Cubic Code Model, Phys. Rev. Lett. **111**, 200501 (2013).

[10] M. B. Ruskai, Pauli Exchange Errors in Quantum Computation, Phys. Rev. Lett. **85**, 194 (2000).

[11] Y. Ouyang, Permutation-invariant quantum codes, Phys. Rev. A **90**, 062317 (2014).

[12] Y. Ouyang and J. Fitzsimons, Permutation-invariant codes encoding more than one qubit, Phys. Rev. A **93**, 042340 (2016).

[13] O. Oreshkov, T. A. Brun, and D. A. Lidar, Fault-Tolerant Holonomic Quantum Computation, Phys. Rev. Lett. **102**, 070502 (2009).

[14] O. Oreshkov, T. A. Brun, and D. A. Lidar, Scheme for fault-tolerant holonomic computation on stabilizer codes, Phys. Rev. A **80**, 022325 (2009).

[15] Y.-C. Zheng and T. A. Brun, Fault-tolerant holonomic quantum computation in surface codes, Phys. Rev. A **91**, 022302 (2015).

[16] M. V. Berry, Quantal phase factors accompanying adiabatic changes, Proc. R. Soc. London A **392**, 45 (1984).

[17] Y. Aharonov and J. Anandan, Phase Change during a Cyclic Quantum Evolution, Phys. Rev. Lett. **58**, 1593 (1987).

[18] F. Wilczek and A. Zee, Appearance of Gauge Structure in Simple Dynamical Systems, Phys. Rev. Lett. **52**, 2111 (1984).

[19] J. Anandan, Non-adiabatic non-abelian geometric phase, Phys. Lett. A **133**, 171 (1988).

[20] P. Zanardi and M. Rasetti, Holonomic quantum computation, Phys. Lett. A **264**, 94 (1999).

[21] J. A. Jones, V. Vedral, A. Ekert, and G. Castagnoli, Geometric quantum computation using nuclear magnetic resonance, Nature (London) **403**, 869 (2000).

[22] L. M. Duan, J. I. Cirac, and P. Zoller, Geometric manipulation of trapped ions for quantum computation, Science **292**, 1695 (2001).

[23] X. B. Wang and K. Matsumoto, Nonadiabatic Conditional Geometric Phase Shift with NMR, Phys. Rev. Lett. **87**, 097901 (2001).

[24] S.-L. Zhu and Z. D. Wang, Implementation of Universal Quantum Gates Based on Nonadiabatic Geometric Phases, Phys. Rev. Lett. **89**, 097902 (2002).

[25] S.-L. Zhu and Z. D. Wang, Unconventional Geometric Quantum Computation, Phys. Rev. Lett. **91**, 187902 (2003).

[26] E. Sjöqvist, D. M. Tong, L. Mauritz Andersson, B. Hessmo, M. Johansson, and K. Singh, Non-adiabatic holonomic quantum computation, New J. Phys. **14**, 103035 (2012).

[27] G. F. Xu, J. Zhang, D. M. Tong, E. Sjöqvist, and L. C. Kwek, Nonadiabatic Holonomic Quantum Computation in Decoherence-Free Subspaces, Phys. Rev. Lett. **109**, 170501 (2012).

[28] G. Feng, G. Xu, and G. Long, Experimental Realization of Nonadiabatic Holonomic Quantum Computation, Phys. Rev. Lett. **110**, 190501 (2013).

[29] C. Zu, W.-B. Wang, L. He, W.-G. Zhang, C.-Y. Dai, F. Wang, and L.-M. Duan, Experimental realization of universal geometric quantum gates with solid-state spins, Nature (London) **514**, 72 (2014).

[30] V. A. Mousolou, C. M. Canali, and E. Sjöqvist, Universal non-adiabatic holonomic gates in quantum dots and single-molecule magnets, New J. Phys. **16**, 013029 (2014).

[31] Z. N. Gürkan and E. Sjöqvist, Realization of a holonomic quantum computer in a chain of three-level systems, Phys. Lett. A **379**, 3050 (2015).

[32] T. Chen, J. Zhang, and Z.-Y. Xue, Nonadiabatic holonomic quantum computation on coupled transmons with ancillaries, Phys. Rev. A **98**, 052314 (2018).

[33] J. Zhang, S. J. Devitt, J. Q. You, and F. Nori, Holonomic surface codes for fault-tolerant quantum computation, Phys. Rev. A **97**, 022335 (2017).

[34] A. M. Stephens, Fault-tolerant thresholds for quantum error correction with the surface code, Phys. Rev. A **89**, 022321 (2014).

[35] D. Colton and R. Kress, Inverse acoustic and electromagnetic scattering theory, SIAM Rev. **36**, 520 (1994).

[36] C. Horsman, A. G. Fowler, S. Devitt, and R. V. Meter, Surface code quantum computing by lattice surgery, New J. Phys. **14**, 123011 (2012).

[37] T. Yamamoto, M. Watanabe, J. Q. You, Yu. A. Pashkin, O. Astafiev, Y. Nakamura, F. Nori, and J. S. Tsai, Spectroscopy of superconducting charge qubits coupled by a Josephson inductance, Phys. Rev. B **77**, 064505 (2008).

[38] J. Q. You, J. S. Tsai, and F. Nori, Controllable manipulation and entanglement of macroscopic quantum states in coupled charge qubits, Phys. Rev. B **68**, 024510 (2003).

[39] J. Q. You, X.-F. Shi, X. Hu, and F. Nori, Quantum emulation of a spin system with topologically protected ground states using superconducting quantum circuits, Phys. Rev. B **81**, 014505 (2010).